Quantum Monte Carlo diagonalization with angular momentum projection

Takahiro Mizusaki,[1] Michio Honma,[2] and Takaharu Otsuka[1,3]
[1]*Department of Physics, University of Tokyo, Hongo, Tokyo 113, Japan*
[2]*Center for Mathematical Sciences, University of Aizu, Tsuruga, Ikki-machi Aizu-Wakamatsu, Fukushima 965, Japan*
[3]*RIKEN, Hirosawa, Wako-shi, Saitama 351-01, Japan*
(Received 7 November 1995)

We present a description of the quantum Monte Carlo diagonalization method. This method has been introduced recently as an approach having both the advantage of the quantum Monte Carlo method and that of the direct diagonalization of the Hamiltonian matrix. In addition, the angular momentum projection is implemented so as to remove the degeneracy with regard to magnetic quantum number. We show that with this method the convergence of the eigenvalues is improved and that the wave functions of excited states can be obtained more easily. Moreover, the calculation of transition matrix elements becomes simpler. [S0556-2813(96)01006-0]

PACS number(s): 21.60.Ka

I. INTRODUCTION

The auxiliary field Monte Carlo technique has been widely used for investigating solid state and nuclear structure physics. This technique enables us to treat the interacting many-body system spanning a Hilbert space with a huge dimension for which the diagonalization of the Hamiltonian cannot be carried out practically. This Monte Carlo technique overcomes the combinatorial complexity of the quantum many-body system and has been successful in describing the zero-temperature and thermal properties of the interacting many-particle system. In nuclear structure physics, Ormand *et al.* have extensively exploited this technique into the nuclear shell model, referring to their method as the shell model Monte Carlo method [1]. However, its application has been rather restricted mainly because of the so-called *minus-sign* problem, a well-known generic and quite difficult problem in the quantum Monte Carlo method. For instance, in the shell model Monte Carlo method, the Hamiltonian must have specific properties with respect to the time-reversal transformation. In addition, the structure of excited states can be partly seen only through response functions. It is crucial to remove such restrictions for further studies of nuclear structure physics at zero temperature.

On the other hand, there is the direct diagonalization method, where the Hamiltonian matrix is diagonalized exactly in an appropriate Hilbert space. In nuclear structure physics, direct diagonalization is widely used and turns out to be a very powerful tool, especially for light nuclei. Owing to the recent development of supercomputers with huge storage and the improvement of algorithms of shell model calculations, direct diagonalization in the large-scale shell model calculation has widen its scope. Recently, there have been some salient developments in the methodology of the shell model diagonalization including stochastic approach. For instance, the stochastic variational method [2] has been proposed by Varga and Liotta who considered that the single-particle basis is stochastically determined utilizing Gaussian-type single-particle wave functions with random oscillator frequencies. In another work, Horoi *et al.* proposed a stochastic truncation method [3] in the shell model diagonalization. Thus, in order to overcome the basis-size problem of the diagonalization of the shell model, the stochastic approach seems promising.

Recently we have proposed a new method which has the aspect of the quantum Monte Carlo method and that of the direct diagonalization. This method has been reported, being referred to as the quantum Monte Carlo diagonalization (QMCD) method [4]. In the QMCD method, appropriate many-body basis states are selected by using the auxiliary field Monte Carlo technique and then diagonalization of the Hamiltonian is carried out with respect to these bases. As an example, we have demonstrated that, by using the interacting boson model (IBM) [5], the basis states obtained in the QMCD method efficiently cover quite well the subspace of the entire Hilbert space which is needed for describing low-lying states. It was shown further [4] that the transition matrix elements among these states can be readily evaluated. Our approach reduces drastically the basis-dimension problem of direct diagonalization, and overcomes certain intrinsic problems of the quantum Monte Carlo method. For instance, we can explicitly access the excited states, and the present method does not suffer from the *minus-sign* problem. We note that, as will be presented elsewhere in detail, the *minus-sign* problem occurs in some shell model Monte Carlo calculations with the IBM Hamiltonian, while the QMCD method works well in such cases. However, basis states obtained in the present method are not eigenstates of angular momentum in general, while the Hamiltonian eigenstates to be obtained are eigenstates of angular momentum. Therefore, the angular momentum is restored stochastically, and degenerate levels of $M=-J,-J+1,\ldots,J-1,J$ are obtained with $J(M)$ being the magnitude (z projection) of the angular momentum. This means that we solve the problem within a redundant space. Moreover, this redundancy prevents us from obtaining more excited states, as discussed later.

As a remedy of the above inefficiency, in the present paper, we propose a new method to incorporate an angular momentum projection into the QMCD method. In general, the full angular momentum projector can be expressed as a three-dimensional integral involving D functions. This projection is difficult for numerical calculation unless the sys-

 © 1996 The American Physical Society

tem has axial symmetry. However, the projection of the z component of the angular momentum suffices in removing the degeneracy with regard to the magnetic quantum number, and is easily incorporated into the QMCD method. It can be carried out by inserting the one-dimensional numerical integration into the computation of overlap and Hamiltonian matrix elements, as we will discuss later. This projection will be referred to naturally as the M projection hereafter. We will report also the efficiency of the M-projected QMCD.

This paper is organized as follows: In Sec. II we sketch the formulation of the QMCD method. In Sec. III, the M-projection method is presented in detail. Section IV is devoted to an illustration of the QMCD method and its M projection by numerical calculations. In Sec. V, we present a summary.

II. FORMULATION OF THE QMCD METHOD

First, we summarize the formulation of the QMCD method [4]. For an illustration, we make use of the IBM as an easily accessible, still yet realistic, many-body system. The boson creation operators are denoted as $b_i^\dagger$ $(i=1,\ldots,N_{\rm sp})$ where $N_{\rm sp}$ denotes the number of single particle states. In the IBM-1, $N_{\rm sp}=6$ and $b_1^\dagger=s^\dagger$, $b_2^\dagger=d_{-2}^\dagger$, $\ldots$, $b_6^\dagger=d_2^\dagger$. The IBM Hamiltonian consists of single-particle energies and a two-body interaction:

$$H=\sum_{i,j=1}^{N_{\rm sp}} \epsilon_{ij} b_i^\dagger b_j+\frac{1}{4}\sum_{i,j,k,l=1}^{N_{\rm sp}} v_{ijkl} b_i^\dagger b_j^\dagger b_k b_l, \tag{1}$$

where ϵ_{ij} and v_{ijkl} are parameters. Presently the QMCD method is a diagonalization of the Hamiltonian matrix with respect to the coherent states created as

$$|\Phi(\vec{x})\rangle=\frac{1}{\sqrt{N_B!}}\left(\sum_{i=1}^{N_{\rm sp}} x_i b_i^\dagger\right)^{N_B}|0\rangle, \tag{2}$$

where $|0\rangle$ is the boson vacuum and the x_i's are (generally complex) amplitudes. N_B denotes the number of bosons. Since the coherent states are nonorthogonal to one another, we solve the generalized linear eigenvalue problem $\mathbf{Hc}=E\mathbf{Nc}$, where $\mathbf{H}$ and $\mathbf{N}$ are the Hamiltonian and norm matrices, which are generally complex. The x_i's are not unique for specifying a given eigenstate of $\mathbf{H}$. No method has been known for selecting the appropriate coherent states efficiently as the basis of diagonalization. Here, in order to select the coherent states, we use the auxiliary field Monte Carlo technique.

In the auxiliary field Monte Carlo method, one of the key technique is the Hubbard-Stratonovich (HS) transformation [6], which allows us to reduce the exponential function of the two-body interactions to the integral of the exponential functions of the linearized one-body fields. In order to perform the HS transformation, it is useful to rewrite the Hamiltonian (1) in a quadratic form

$$H=\sum_{\alpha=1}^{N_f}(E_\alpha O_\alpha+\tfrac{1}{2}V_\alpha O_\alpha^2), \tag{3}$$

where O_α's and N_f denote one-body operators and the number of one-body operators, respectively. The N_f can be at most $N_{\rm sp}^2$ and usually appears to be much smaller. The E_α and V_α are coefficients deduced from Eq. (1).

By dividing the imaginary time β into N_t steps, the imaginary time evolution operator (many-body propagator) $e^{-\beta H}$ can be written as the product of time-sliced imaginary time evolution operators:

$$e^{-\beta H}=\prod_{n=1}^{N_t} e^{-\Delta\beta H}, \tag{4}$$

where $\Delta\beta=\beta/N_t$. By applying the HS transformation to each time step [7], this operator can be expressed as an integral of one-body evolution operators (one-body propagators) with respect to the auxiliary fields $\sigma_{\alpha n}$:

$$e^{-\beta H}\approx\int_{-\infty}^{\infty}\prod_{\alpha,n} d\sigma_{\alpha n}\left(\frac{\Delta\beta|V_\alpha|}{2\pi}\right)^{1/2} G(\sigma)\prod_n e^{-\Delta\beta h(\vec{\sigma}_n)}, \tag{5}$$

where $\vec{\sigma}_n$ means a set of auxiliary fields of the nth time step, $\vec{\sigma}_n=(\sigma_{1n},\sigma_{2n},\ldots,\sigma_{N_f n})$, and σ denotes the assembly of the auxiliary fields over all the time steps, $\sigma=\{\vec{\sigma}_1,\vec{\sigma}_2,\ldots,\vec{\sigma}_{N_t}\}$. The Gaussian weight factor $G(\sigma)$ is defined by

$$G(\sigma)=\exp\left(-\sum_{\alpha,n}\frac{\Delta\beta}{2}\left|V_\alpha\right|\sigma_{\alpha n}^2\right), \tag{6}$$

and $h(\vec{\sigma}_n)$ is one-body Hamiltonian defined by

$$h(\vec{\sigma}_n)=\sum_\alpha (E_\alpha+s_\alpha V_\alpha\sigma_{\alpha n})O_\alpha, \tag{7}$$

where $s_\alpha=\pm 1$ $(=\pm i)$ if $V_\alpha<0$ (>0). The operator (5) is a ground state projector acting on the trial state which has nonvanishing overlap with the ground state, that is,

$$\lim_{\beta\to\infty} e^{-\beta H}|\Phi^{(0)}\rangle\propto|\Phi_g\rangle, \tag{8}$$

where $|\Phi_g\rangle$ denotes the ground state and the $|\Phi^{(0)}\rangle$ is an initial wave function. In the case of the present calculation, $|\Phi(\vec{x})\rangle$ with an appropriate initial $\vec{x}$ can be $|\Phi^{(0)}\rangle$.

In principle, the multidimensional integration in Eq. (5) can be evaluated by the Monte Carlo method where σ is taken from the Gaussian random number distribution with the weight function (6). Each set of σ yields the corresponding $|\Phi(\sigma)\rangle$:

$$|\Phi(\sigma)\rangle\propto\prod_{n=1}^{N_t} e^{-\Delta\beta h_n(\sigma)}|\Phi^{(0)}\rangle. \tag{9}$$

For one set of σ, the one-body evolution operator (9) can be considered to be a transformation from an initial $|\Phi^{(0)}\rangle$ to a final $|\Phi(\sigma)\rangle$ which is also a coherent state. Therefore, the exact ground state can be expressed by a linear combination of the many coherent states generated by the corresponding auxiliary fields σ's. The auxiliary field quantum Monte Carlo method implicitly and stochastically ensures the cor-

rect linear combination of such coherent states for the ground state. In the QMCD method, as discussed below, the linear combination is determined explicitly by diagonalizing the Hamiltonian in a subspace formed by selected coherent states.

Each coherent state which contains the large fraction of the wave function of the ground state can be considered to be a good basis vector for describing the low-lying states, and the one-body evolution operator (9) generates such coherent states, as we will discuss later. In this sense, the one-body evolution operator (9) can be considered to be a generator of bases for describing the low-lying states in a good approximation, in contrast with the fact that the many-body propagator $e^{-\beta H}$ is an exact ground-state projector. Therefore, we can use these coherent states as the bases for diagonalizing the Hamiltonian matrix. We note that we can use different initial states if necessary, for instance, in the case of the shape coexistence problem. The different sets of random numbers provide different σ auxiliary fields and consequently different coherent basis states. Because such coherent states are nonorthogonal and can be similar to each other, we orthogonalize them. Moreover, we select the *good* bases by the perturbative estimation in the sense of ''stochastic diagonalization'' [10] as we will discuss later. Thus, we increase the bases in diagonalizing the Hamiltonian matrix until the obtained energies converge. In the previous paper [4], we have shown that this procedure works well, and that we end up with well-convergent energies and wave functions for several low-lying states. The QMCD method is composed of two processes: One is the generation of the bases (i.e., QMCD bases) for describing the low-lying states by the auxiliary field Monte Carlo technique, and the second is the diagonalization process in terms of the QMCD bases. It is important to realize that the bases are automatically selected by the dynamics of the system in the former process, and, in this sense, we diagonalize the Hamiltonian in the full space (no space truncation).

III. ANGULAR MOMENTUM PROJECTION METHOD

In this subsection, we present a prescription for removing the degeneracy with regard to magnetic quantum number. In order to extract the component of a given magnetic quantum number M from the coherent state, we introduce the state

$$|\Phi(\sigma,M)\rangle = P_M|\Phi(\sigma)\rangle = \frac{1}{2\pi}\int_0^{2\pi} d\phi e^{-i\phi(J_z-M)}|\Phi(\sigma)\rangle, \tag{10}$$

where P_M is the projector onto the total magnetic quantum number M. Here J_z stands for the z component of angular momentum operators. Note that J_z is an operator and M is its quantum number. The state $|\Phi(\sigma,M)\rangle$ will be referred to as the M-projected coherent state. The corresponding overlap and matrix element of the Hamiltonian are evaluated with one-dimensional integration over ϕ in Eq. (10). The numerical calculation for the M projection is easier in comparison to the full angular momentum projection.

If we consider the states with angular momentum J, we can use the M-projected coherent states with $M=J$. The subspace with the definite total magnetic quantum number $M=J$ is often used in shell model diagonalization in the m scheme. As this space certainly includes eigenstates with angular momenta higher than J, we add the $J\cdot J$ term to the Hamiltonian, so as to push up the eigenstates with higher angular momenta. Hence, with this procedure, we can obtain low-lying states with the angular momentum J, separating them from other states with different angular momenta. With regard to the $J\cdot J$ term, the same technique has been used for stabilizing the numerical calculation in the m-scheme diagonalization. In this respect, the present M projection has a certain similarity to the shell model diagonalization in the m scheme.

We summarize the procedure of the M-projected QMCD method.

(1) We take an initial coherent state which is supposed to contain the low-lying states to be obtained.

(2) A set of the auxiliary fields σ is given stochastically according to the Gaussian weight function (6).

(3) We calculate a wave function $|\Phi(\sigma)\rangle$ for the present set σ.

(4) The M projection is carried out by the projection operator (10). The presently obtained M-projected coherent state $|\Phi(\sigma,M)\rangle$ is orthonormalized by means of the Schmidt method with respect to all other basis states obtained previously, and then a new basis state $|\Phi'(M)\rangle$ added to the basis states is determined. In order to accelerate the convergence, we use the following criterion for selecting *good* bases [10]. The energy decrease ΔE which originates in the new basis state $|\Phi'(M)\rangle$ can be estimated by

$$\Delta E \sim \sum_{i=1}^{N_e} \frac{1}{2}\{E_i-\varepsilon+\sqrt{(E_i-\varepsilon)^2+4|D_i|^2}\}, \tag{11}$$

where N_e is the number of the eigenstates which we try to solve, E_i denotes the energy of the ith state obtained in the previous step, $\varepsilon=\langle\Phi'(M)|H|\Phi'(M)\rangle$, and $D_i=\langle\Psi_i|H|\Phi'(M)\rangle$ where Ψ_i is the ith wave function obtained in the previous step. If ΔE is small, for example, less than 10% in comparison to the energy decrease in the previous steps, the state $|\Phi'(M)\rangle$ is discarded, and we return to step (2).

(5) By adding the new basis state obtained in step (4) to the subspace where the Hamiltonian H is diagonalized, we obtain improved energies E_i's of the considered states and their wave functions $|\Psi_i\rangle$ $(i=1,\ldots,N_e)$.

(6) The steps from (2) to (5) are repeated until the energies E_i's of the considered states converge.

The present angular momentum projection is carried out only in the diagonalization process. We do not apply any modification to the Monte Carlo procedure. However, because the coherent state generated by the imaginary time evolution operator (9) contains various angular momenta, the M-projected basis can be considered to be good as a basis for the subspace with a given magnetic quantum number. Moreover, the M projection reduces the burden of the diagonalization by decreasing the dimension.

The M projection has been studied also in the shell model Monte Carlo method [8]. Moreover, the angular momentum projection of the path integral representation of the partition function has been proposed by Rossignoli and Ring [9].

They discussed the general projected statistics of a grand canonical ensemble according to the symmetry of the Lie algebra, and showed the importance of such an angular-momentum-projected calculation within the static path approximation.

The present method is different from the above-mentioned approaches, particularly in the aspect that the present M projection is plugged into the diagonalization process. Thus, the M-projected QMCD method is somewhat related to shell model diagonalization in the m scheme with similar projection procedures.

IV. ILLUSTRATIONS BY NUMERICAL CALCULATIONS

A. IBM Hamiltonian

In the following, the M-projected QMCD method is applied to the O(6) limit of the sd-IBM and the SU(3) limit of the sdg-IBM [5] as a demonstration. The O(6) and SU(3) limits of the IBM represent the γ-unstable and axially symmetric deformed nuclei, respectively. The sdg-IBM is an extension of the sd-IBM by including the hexadecupole degree of freedom and can be more suitable in describing certain aspects of well-deformed nuclei. As the cases of the SU(3) and O(6) limits describe deformed nuclei, almost the entire space is needed to diagonalize the Hamiltonian in the spherical [i.e., U(5)] basis and hence there is no appropriate truncation scheme. Because the Hilbert space of the sdg-IBM is quite huge, the present method is useful for solving the Hamiltonian. We start with the IBM Hamiltonian

$$H = -\kappa Q\cdot Q + \kappa' J\cdot J, \tag{12}$$

where J represents the angular momentum operator and Q is the quadrupole operator defined by

$$Q = s^{\dagger}\tilde{d} + d^{\dagger}s + \chi[d^{\dagger}\tilde{d}]^{(2)} + \lambda[d^{\dagger}\tilde{g} + g^{\dagger}\tilde{d}]^{(2)} + \omega[g^{\dagger}\tilde{g}]^{(2)}. \tag{13}$$

In the case of the O(6) limit of the sd-IBM, χ, λ, and ω vanish. The SU(3) limit of the sdg-IBM can be obtained with $\chi = -11\sqrt{10}/28$, $\lambda = 9/7$, and $\omega = -3\sqrt{55}/14$.

B. Comparison between QMCD and M-projected QMCD methods

First we present the results of the QMCD method without the M projection. As we have already mentioned, the resultant eigenstates are degenerate with respect to the magnetic quantum number M. For instance, the fivefold 2_1^+ level appears in the QMCD calculation. Figure 1 shows the convergence pattern of several low-lying levels by open diamonds. The levels come down basically as the dimension of the subspace spanned by the QMCD basis states is increased. This dimension is called the QMCD basis dimension. We show the convergence of the eigenvalues for up to the eighth level as a function of the QMCD basis dimension. We show the cases of the SU(3) and O(6) limits. We observe the fivefold degeneracy with regard to the magnetic quantum number of the 2_1^+ level in both cases. The boson number is taken to be 16. Other parameters are given in the figure caption. Since the dimension in the full sdg space turns out to be

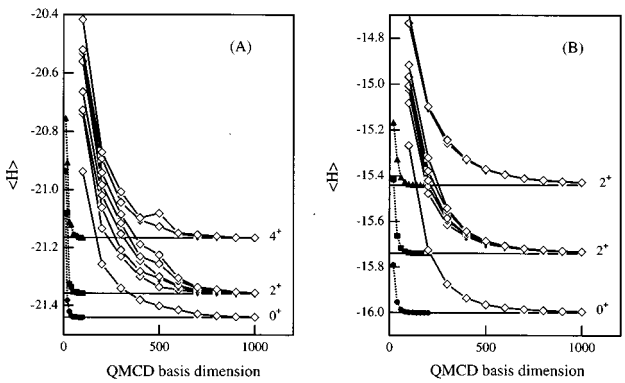

FIG. 1. Excitation energies of the low-lying states for the results of QMCD (open diamond) and M-projected QMCD (solid circle, square, and triangle) methods as a function of the QMCD basis dimension. The points are connected to guide the eyes. The Hamiltonian is taken as the SU(3) limit for (A) and the O(6) limit for (B). Other parameters used are $\Delta\beta = 16$, $N_t = 20$, $\kappa = 0.1$, and $\kappa' = 0.01$. The exact values are also shown by horizontal lines. In the case of the QMCD method, we show the results for up to the eighth level.

155 117 520 in this sdg calculation, we see the remarkable efficiency of the QMCD calculation over the direct diagonalization.

The degeneracy with respect to magnetic quantum number means that we solve the Hamiltonian in a redundant way. As described above, the M-projection technique removes this redundancy by lifting the degeneracy. Solid symbols in Fig. 1 indicate the convergence pattern of certain lowest levels obtained with the M projection. In fact, we show the results of the QMCD calculation with the M projection onto the $M = 0$ space. The corresponding m-scheme dimension (with $M = 0$) is 4 859 194 for the sdg-IBM. As we decompose the whole space into subspaces with definite magnetic quantum number, the dimension of the considered Hilbert space is reduced significantly. In order to compare the efficiency of convergence in the QMCD method with that in the M-projected QMCD method, we show the results using the same parameters of the Hamiltonian. Since the results with and without the M projection are included in Fig. 1, one finds that the efficiency of the M-projected QMCD method for the O(6) and SU(3) limits is quite high compared to the QMCD method without the M projection. In the QMCD method without the M projection, since the eigenstates are degenerate with respect to magnetic quantum number, a larger QMCD basis dimension is needed to complete such multiplets of a given J. Moreover, in the QMCD method without the M projection, it is difficult to obtain higher excited states, because basically all the eigenstates below the state of the interest have to be obtained. In turn, in the M-projected QMCD method, this difficulty is removed. As a consequence, we can easily handle many excited states with various angular momenta. From this comparison, one concludes that the M projection plays a very important role in the practical calculations. In the following, we discuss detailed properties of the M-projected QMCD calculation.

C. Statistical property of the QMCD basis

Here we take a boson number $N_B = 30$. While this is larger than usual values, this is chosen only for the sake of

examination of the efficiency of the present method. In the case of the sdg-IBM, the m-scheme basis dimension with $M=0$ turns out to be 2 332 164 293, for which the full diagonalization is much beyond the scope of any computer available in the near future.

Before proceeding to the results of the QMCD method, we discuss certain properties of the coherent states obtained by the one-body operator (9). This operator is of the form of the imaginary time evolution, and its function in Eq. (5) is very clear. However, since it contains not the original Hamiltonian H but the one-body operator h [see Eq. (7)] obtained from H, the meanings of the operator in Eq. (9) should be clarified. We take an initial state and trace its evolution by Eq. (9). The evolution is carried out by time slice $\Delta\beta$, which is repeated N_t times, giving rise to $\beta=\Delta\beta N_t$. The values $N_t=20$ is taken. We first examine the variation of the energy expectation value of the state $|\Phi(\sigma)\rangle$. Here we keep N_t unchanged but vary $\Delta\beta$, which results in different β, because of $\beta=\Delta\beta N_t$. For a given value of β (or $\Delta\beta$), we repeat stochastically the evolution process in Eq. (9) with $N_{\rm sig}$ sets of randomly selected σ's. We take $N_{\rm sig}=400$ in the present calculation. The energy expectation value $E(\sigma,\beta)$ is then calculated for each β and each set of σ as

$$E(\sigma,\beta)=\frac{\langle\Phi(\sigma)|HP_M|\Phi(\sigma)\rangle}{\langle\Phi(\sigma)|P_M|\Phi(\sigma)\rangle}. \tag{14}$$

Note that the M projection is made. Thus, we obtain $N_{\rm sig}$ values for each value of β. We then consider the average and standard deviation of E in Eq. (14) with respect to σ:

$$\overline{E(\beta)}=\frac{1}{N_{\rm sig}}\sum_{\sigma}E(\sigma,\beta), \tag{15}$$

$$\Delta E(\beta)=\left\{\frac{1}{N_{\rm sig}}\sum_{\sigma}[E(\sigma,\beta)-\overline{E(\beta)}]^2\right\}^{1/2}. \tag{16}$$

The values of the average $\overline{E(\beta)}$ and the standard deviation $\Delta E(\beta)$ are shown in Fig. 2 as functions of β $(=\Delta\beta N_t)$ for $M=$ 0, 4, and 6. In the QMCD description, an eigenstate is expressed in terms of stochastically generated bases which are actually M-projected states $|\Phi(\sigma,M)\rangle$ in Eq. (10). Low-lying eigenstates are described by a given set of such basis states to almost the same extent. Therefore, the $M=$ 0, 4, and 6 states in Fig. 2 show similar patterns. As $\Delta\beta$ increases, the average energy decreases, and for $\Delta\beta\geqslant 25$ $(\beta\geqslant 500)$ it reaches an almost constant value. On the other hand, in Fig. 2, we can see that the variance of the energy does not decrease as β increases. Since this variance is a consequence of a certain variety of the states in Eq. (10), this property can be utilized in the QMCD method for generating many linearly independent QMCD bases at a definite value of β. Therefore, we can see that the one-body evolution operator (9) works as a projector for extracting states in Eq. (10), needed as bases for low-lying states. This is a very useful property.

At smaller β, the coherent states in Eq. (9) have higher energy expectation values. Hence, we can anticipate that such coherent states contain a larger fraction of excited eigenstates. At a certain β, by the auxiliary field Monte Carlo technique, we can obtain many coherent states within the aforementioned variance. After obtaining all the available coherent states at a certain β, we can thus obtain another set of coherent states if we decrease β. We use this property in selecting the QMCD basis.

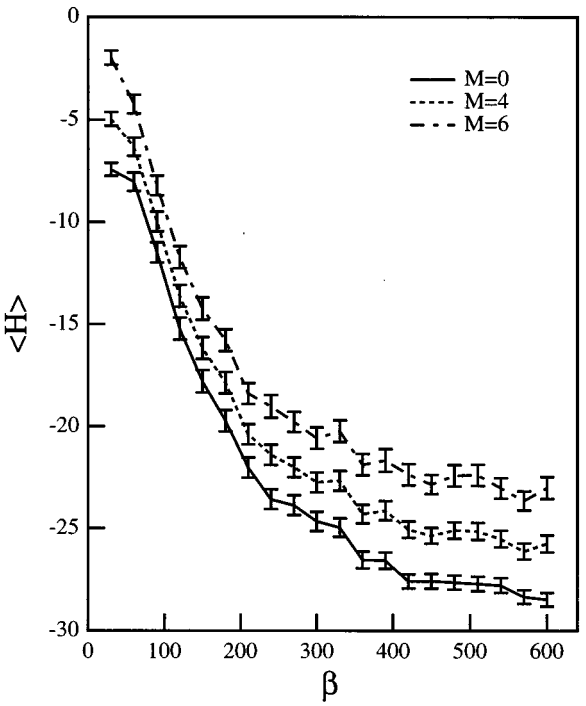

FIG. 2. Average energies and variances of the QMCD bases as a function of β. The average energy and variance are calculated with the 400 coherent states for $M=0$, 4, and 6 space at each β. The variances are indicated by the error bars. The Hamiltonian of the exact SU(3) limit is taken. The parameters used are $N_B=30$, $N_t=20$, $\kappa=0.005$, and $\kappa'=0.05$.

Finally, we note that the inverse temperature β in the present work has no physical meaning and it is used as a mathematical tool because we work in the framework of the microcanonical ensemble (zero-temperature formalism).

D. SU(3) limit

Next we discuss detailed feature of the M-projected QMCD method in the case of the SU(3) limit. Figure 3 shows the energies and the expectation values of $J\cdot J$ as functions of the QMCD basis dimension, for $M=0$. The adopted values of other parameters are given in the figure caption. One sees that the yrast energies of 0_1^+, 2_1^+, 4_1^+, and 6_1^+ converge within the QMCD basis dimension of about 50. On the other hand, nonyrast states show a clearly different and slower convergence. The members of the β and γ bands, 0_2^+, 2_2^+, 2_3^+, 3_1^+, and 4_2^+, require QMCD bases of about 350 for convergence of the energy and of the $J\cdot J$ value.

Figure 4(A) shows the energies of the yrast and several nonyrast excited states as functions of the QMCD basis dimension for the $M=4$ space. Obviously, the 0^+ and 2^+ levels are absent in Fig. 4. Because of the elimination of the 0^+ and 2^+ states, we can obtain the 4_2^+ and 4_3^+ states much more easily than in the $M=0$ space. One can see the degeneracy of the 4_2^+ and 4_3^+ states, which is characteristic in the SU(3) limit. Comparing Fig. 3 to Fig. 4, we can see that

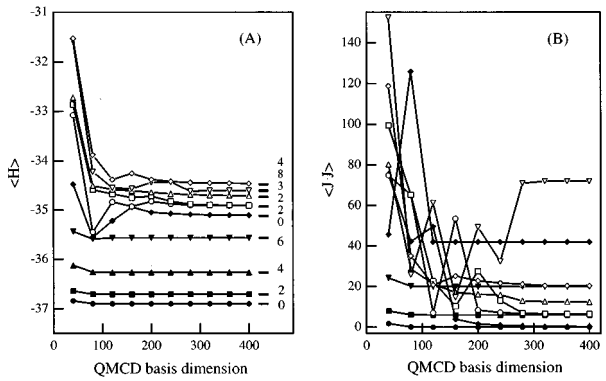

FIG. 3. (A) Energies and (B) expectation values of the angular momentum of low-lying states as functions of the QMCD basis dimension. The $M=0$ space is considered. The Hamiltonian of the exact SU(3) limit is taken. The parameters used are $N_B=30$, $N_t=20$, $\kappa=0.005$, $\kappa'=0.03$, and initial $\Delta\beta=25$. The exact values are shown by horizontal bars.

levels are displaced. This is due to strength of a repulsive $J\cdot J$ interaction, which is larger in the calculation shown in Fig. 4. The adopted values of the parameters are given in the figure caption. These figures show that the M-projected QMCD method can reproduce not only the yrast states but also the members of the β and γ bands.

An axially symmetric coherent state $(\lambda^\dagger)^{N_B}|0\rangle$, where $\lambda^\dagger=\Sigma_l x_l b_{l0}^\dagger$, gives the exact wave function in the SU(3) limit after projecting it onto a good angular momentum. Here the x's are amplitudes, while the b's stand for bosons. This can be achieved by projecting the above coherent state with an appropriately chosen λ. This means that a coherent state is a good basis for the yrast states in the SU(3) limit.

Concerning the members of the β and γ bands, it may be useful to consider the Tamm-Dancoff approximation (TDA) in boson systems, where the intrinsic states are of the form $b_{lm}^\dagger(\lambda^\dagger)^{N_B-1}|0\rangle$. We now discuss how to generate such states in the QMCD method.

We consider two coherent states resembling each other. These coherent states are denoted by $(\lambda_i^\dagger)^{N_B}|0\rangle$ $(i=1,2)$ where $\lambda_i^\dagger=\Sigma_{lm}x_{ilm}b_{lm}^\dagger$ $(i=1,2)$. In the case of $\lambda_1\sim\lambda_2$, the $(\lambda_2^\dagger)^{N_B}|0\rangle$ is shown as $(\lambda_1^\dagger+\delta\lambda^\dagger)^{N_B}|0\rangle \sim(\lambda_1^\dagger)^{N_B}|0\rangle +N_B\delta(x_{1lm})b_{lm}^\dagger(\lambda_1^\dagger)^{N_B-1}|0\rangle+\cdots$. After the Schmidt orthgonalization, the first component on the right-hand side disappears. The remaining component is basically the generalized TDA trial wave function. Thus, in the QMCD method, TDA(-like) states are included, by varying the λ's. This is why the QMCD method can easily produce the β and γ bands.

E. O(6) limit

The O(6) limit represents γ-unstable deformed nuclei. Recently, the structure of O(6) nuclei has been reinterpreted as a multiphonon scheme built on the γ-unstable deformed ground state [11]. As this structure is not simpler than that of the SU(3) from the viewpoint of the coherent state, this is a good testing ground to see whether or not the QMCD method can reproduce eigenenergies and eigenstates. Here, we add to the Hamiltonian (12) the interaction $\kappa_3 T^{(3)}\cdot T^{(3)}$, where $T^{(3)}=[d^\dagger\tilde{d}]^{(3)}$. As $T^{(3)}\cdot T^{(3)}$ is a Casimir operator of O(5), the Hamiltonian remains in the O(6) limit and can be still solved algebraically. However, it increases the number of auxiliary fields. In Fig. 5, we show the energy and the expectation value of $J\cdot J$. Contrary to the convergence pattern of the SU(3) limit shown in Fig. 4, the convergence patterns of yrast levels are very similar to that of nonyrast levels as functions of the QMCD basis dimension. This is because yrast and nonyrast states of O(6) have equally complicated intrinsic structures. We can calculate the Hamiltonian matrix for the space with a fixed value of M. This space includes the levels with $J\geqslant M$. In order to separate states of $J>M$ from those of $J=M$, we add the $J\cdot J$ term to the Hamiltonian. In Fig. 6(A), we show the results of the $M=6$ space. In this case, we evaluate six well-convergent 6^+ levels by using the $J\cdot J$ term. Thus, the M projection with a large $J\cdot J$ term works efficiently, making it possible that a decent number of low-lying levels of the deformed nuclei can be obtained.

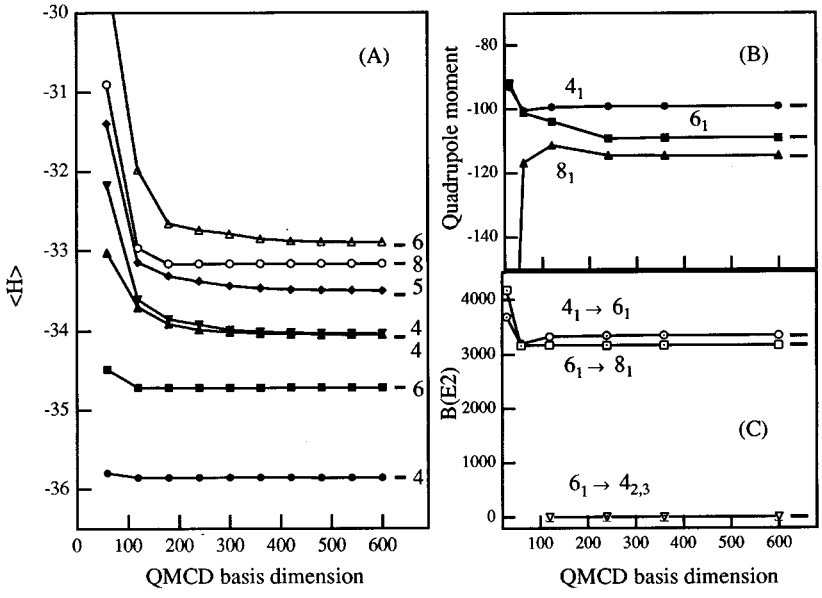

FIG. 4. (A) Energies of the low-lying states, (B) quadrupole moments of yrast states, and (C) several $B(E2)$'s as functions of the QMCD basis dimension. The $M=4$ space is considered. The Hamiltonian of the exact SU(3) limit is taken. The parameters used are $N_B=30$, $N_t=20$, $\kappa=0.005$, $\kappa'=0.05$, and initial $\Delta\beta=8$. The exact values are shown by horizontal bars.

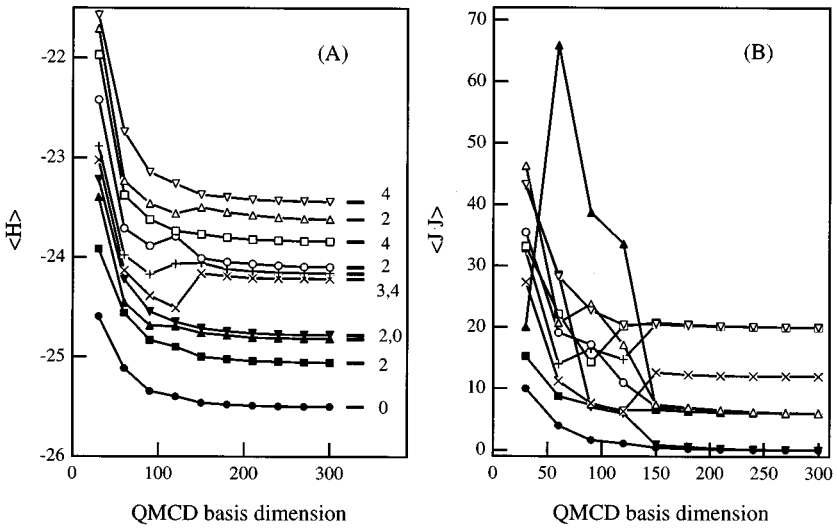

FIG. 5. (A) Energies and (B) expectation values of the angular momentum of the low-lying states as functions of the QMCD basis dimension. The $M=0$ space is considered. The Hamiltonian of the exact O(6) limit is taken. The parameters used are $N_B=30$, $N_t=20$, $\kappa=0.025$, $\kappa_3=0.03$, $\kappa'=0.05$, and initial $\Delta\beta=10$. The exact values are shown by horizontal bars.

F. Basis-size problem of the QMCD method

One of the advantages of the auxiliary field quantum Monte Carlo method is that, due to the linearized one-body Hamiltonian by the HS transformation, the size of the required space for the numerical calculation for the many-particle system is reduced to that of a single-particle one, independent of the number of particles involved in the considered system. Therefore, the shell model Monte Carlo method overcomes the basis-size problem of direct diagonalization. On the other hand, the QMCD method is a combination of the auxiliary field quantum Monte Carlo method and the direct diagonalization method. Therefore, the QMCD method may inherit their advantages and disadvantages. As the QMCD method spans the bases of the diagonalization, there is a possibility that the dimension of required QMCD bases may be too large. It is important to investigate the relation between the QMCD basis dimension and the dimension of the entire Hilbert space as functions of the number of particles involved, because it determines the scope of the application of the present method.

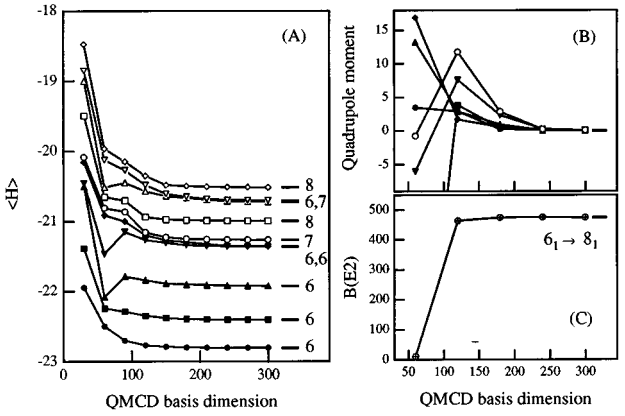

FIG. 6. (A) Energies of the low-lying states, (B) quadrupole moments of up to the sixth state, and (C) $B(E2;\, 6_1^+ \rightarrow 4_1^+)$ as functions of the QMCD basis dimension. The $M=0$ space is considered. The Hamiltonian of the exact O(6) limit is taken. The parameters used are $N_B=30$, $N_t=20$, $\kappa=0.025$, $\kappa_3=0.03$, $\kappa'=0.05$, and initial $\Delta\beta=10$. The exact values are shown by horizontal bars.

In the QMCD method, by construction, the bases are determined by the mean fields which are generated in a stochastic way, and hence the basis size is mainly dependent on the number of the mean fields dominating the structure of the states of interest. On the other hand, the dependence of the boson number can be expected to be indirect and weak. In Table I, we show the typical values of QMCD basis dimension required for having convergence of the 0_1^+ states in the case of the SU(3) and O(6) limits. The corresponding m-scheme dimension of the entire Hilbert space grows rapidly from 10^2 to 10^9 as the boson number increases. On the other hand, in the QMCD, the required dimension of the QMCD basis is rather independent of boson number. However, it depends on the property of the Hamiltonian of the considered system. One can see that in the application to the IBM, the QMCD method has a significant advantage in the basis-size problem over the direct diagonalization method.

G. Transition matrix elements

In the shell model Monte Carlo method, the excited states can be studied through the response function [1]. Some of the transition matrix elements can be estimated by this response function. In turn, in the QMCD method, owing to the introduction of the diagonalization process, we can explicitly construct the wave functions of the excited states. As a consequence, we can easily compute the transition matrix elements.

TABLE I. QMCD basis dimension needed for the convergence for the 0_1^+ level as a function of boson number N_B. The dimension of the full $M=0$ subspace is listed for comparison. The SU(3) and O(6) limits are considered. The convergence of each state is judged by $\langle J\cdot J\rangle \leqslant 0.01$, where J is the angular momentum operator.

	SU(3)		O(6)	
N_B	QMCD basis	Full $M=0$	QMCD basis	Full $M=0$
10	30	92123	60	202
20	50	39180981	130	1957
30	70	2332164293	230	8265

For evaluating the transition matrix elements between the low-lying excited states, eigenstates with definite J and M are needed. In a previous paper [4], for improving the separation of the degenerate eigenstates with different M's, we modified the Hamiltonian by adding the term $\gamma(J_z-M)^2$. Obliviously, we take a positive γ and some integer M. With this term, all states with $J_z \neq M$ can be pushed up. However, as the $\gamma(J_z-M)^2$ term makes the convergence worse, a large dimension of the QMCD basis is required. On the contrary, due to the M projection, such a problem does not arise in the present approach.

In Figs. 4(B) and 6(B), we show the convergence of the quadrupole moment of each state as functions of the QMCD basis dimension. In the case of the O(6) limit, the quadrupole moments of all the states should vanish. Figure 6(B) confirms this property as the QMCD basis dimension increases. In Figs. 4(C) and 6(C), we show the convergence of the $B(E2)$ values as functions of the QMCD basis dimension. In these figures, the quantum numbers of angular momentum and its z component are assigned approximately, for the cases where convergence is not achieved. In the case of the SU(3) limit, the interband $B(E2)$'s vanish while the intraband $B(E2)$'s have large values. Figure 4(C) shows that these features are accomplished as functions of the QMCD basis dimension. By showing the convergence of the quadrupole moment and $B(E2)$, we can confirm the convergence of the wave function obtained by the QMCD method.

We finally make remarks on the computational aspect of the transition matrix element calculation. The coherent states span the over complete space as we have already mentioned. The same wave function can be represented in many ways. For instance, a different initial seed of the random number gives rise to a completely different representation of the same wave function because the present method is purely stochastic. Moreover, the wave function of a given J can be manipulated in various subspaces with different magnetic quantum numbers. Therefore, to evaluate the transition matrix elements, we have several methods of computation. However, if the initial and final wave functions are represented by the same bases, it is most convenient for the calculation of the transition matrix elements, because the reevaluation of the norm matrix is not needed.

V. SUMMARY

In summary, we have sketched the QMCD method that we have recently proposed [4]. We have explained that the QMCD method has the advantages of both the quantum Monte Carlo method and the conventional diagonalization method often used in shell model calculations. The application of the QMCD method provides us with quite accurate eigenvalue solutions within the tractable number of the QMCD basis dimensions. However, it produces degenerate eigenstates with respect to the magnetic quantum number. Hence, we have introduced the M-projection method into the QMCD method. This M projection reduces the Hilbert space by decomposing it into subspaces with definite magnetic quantum numbers. This is a method analogous to the shell model diagonalization in the m scheme. Contrary to the full angular momentum projection, the present method is easy for numerical calculations. By this projection method, convergence of the eigenvalues is extremely improved. The degeneracy with respect to the magnetic quantum number is removed. As a consequence, we can easily evaluate the properties of excited states. After diagonalization of the Hamiltonian, the resultant wave function has a definite angular momentum and z projection, if the convergence is achieved. This makes the evaluation of the transition matrix elements easier. The present M-projection method seems to be an indispensable tool for applying the QMCD method to nuclear structure physics.

Up to now, we have discussed numerical examples by utilizing the group theoretical limits of the IBM, for the sake of comparison to exact solutions. For systems with a boson number as large as $N_B \sim 20-30$, it is impossible to diagonalize the full IBM Hamiltonian. However, we have confirmed that in the present method the QMCD basis dimension needed for reasonable convergence is tractable also for other more general Hamiltonians.

We are now trying to apply this method to fermion systems. The significant improvement in the boson system suggests that this M-projected QMCD method should work in fermion systems as well.

ACKNOWLEDGMENTS

One of the authors (M.H.) would like to thank Dr. H. Nakada for discussions. This work was supported in part by a Grant-in-Aid for Scientific Research on Priority Areas (No. 05243102) from the Ministry of Education, Science and Culture. A part of the computation for this work was carried out on the VPP500 computer at RIKEN as a research program in the Computational Nuclear Physics Project of RIKEN.

[1] W.E. Ormand, *et al.*, Phys. Rev. C **49**, 1422 (1994); C.W. Johnson *et al.*, Phys. Rev. Lett. **69**, 3147 (1992).
[2] K. Varga and R.J. Liotta, Phys. Rev. C **50**, R1292 (1994).
[3] M. Horoi, B.A. Brown, and V. Zelevinsky, Phys. Rev. C **50**, R2274 (1994).
[4] M. Honma, T. Mizusaki, and T. Otsuka, Phys. Rev. Lett. **75**, 1284 (1995).
[5] F. Iachello and A. Arima, *The Interacting Boson Model* (Cambridge University Press, Cambridge, England, 1987).
[6] J. Hubbard, Phys. Lett. **3**, 77 (1959); R.D. Stratonovich, Dokl. Akad. Nauk. SSSR **115**, 1907 (1957) [Sov. Phys. Kokl. **2**, 416 (1958)].
[7] M. Suzuki, Commun. Math. Phys. **51**, 183 (1976).
[8] H. Nakada and Y. Alhassid (private communication).
[9] R. Rossignoli and P. Ring, Ann. Phys. (N.Y.) **235**, 350 (1994).
[10] H. De Raedt and M. Frick, Phys. Rep. **231**, 107 (1993).
[11] T. Otsuka and K.H. Kim, Phys. Rev. C **50**, R1768 (1994); G. Siems *et al.* Phys. Lett. B **320**, 1 (1994).